KYBERNETIKA — VOLUME *46* (2010), NUMBER 5, PAGES 907–925

OPTIMAL BOUNDARY CONTROL FOR HYPERDIFFUSION EQUATION

Hanif Heidari and Alaeddin Malek

In this paper, we consider the solution of optimal control problem for hyperdiffusion equation involving boundary function of continuous time variable in its cost function. A specific direct approach based on infinite series of Fourier expansion in space and temporal integration by parts for analytical solution is proposed to solve optimal boundary control for hyperdiffusion equation. The time domain is divided into number of finite subdomains and optimal function is estimated at each subdomain to obtain desired state with minimum energy. Proposed method has high flexibility so that decision makers are able to trace optimal control in a prescribed subinterval. The implementation of the theory is presented and the effectiveness of the boundary control is investigated by some numerical examples.

Keywords: hyperdiffusion equation, optimal boundary control, swimming at microscale

Classification: 35K35, 35B37, 49J20

1. INTRODUCTION

There exist many swimming microorganisms in our world. Some examples are: The spermatozoon that fuse with the ovum during fertilization, the bacteria that inhabit our guts, the protozoa in our ponds, and the algae in the ocean [13]. The hair-like filaments called flagella that build the tail of spermatozoa generate thrust by passing bending waves from head to tail along the filament. Similarly, cilia are whip-like appendages which pump fluid using an asymmetric beating cycle. In the case of motile cells, this transport of fluid also leads to propulsion [2]. What is perhaps less familiar is the fact that the physics governing swimming at the micron scale is fundamentally different from the physics of swimming at the mesoscopic scale. The world of microorganisms is the world of low "Reynolds number," a world where inertial forces are less significant or even negligible compared to viscous forces [19]. If w denotes the typical amplitude of a material point at a distance x along the filament, the balance between local viscous drag and bending forces on the filament results in a hyperdiffusion equation for small-amplitude motion. This equation was also derived in earlier work by Machin in the context of wave propagation in the flagella of swimming microorganisms [15, 16].

There exist some experimental works on swimming in microscale. The first artificial microswimmer is created by Dreyfus et al. in which a chain of paramagnetic

beads propagates a bending wave along the chain driven by an external magnetic field [6]. A second experiment performed by Wiggins et al. measured the shape changes of a passive actin filament, oscillated at one end via optical tweezers [23]. The shapes recorded in these trials match elastohydrodynamic theory well. Microswimmers could provide propulsion for medical device used for minimally invasive surgery or targeted drug delivery. Also, microswimmers could easily be adopted to work as a micro-electro-mechanical-system (MEMS) pumps for "lab on chip" applications [11].

Optimal control is one of the methods that is applied to many problems to achieve desired state with minimum energy [24]. Although there are many publications on first and second order problems [5, 7, 10, 17, 18, 20, 22], there is little research on boundary control for fourth order hyperdiffusion equations. This paper deals with optimal boundary control of hyperdiffusion equation. We consider a microfilament with both ends are hinged. Our goal is to find the control function which acts on the extreme $x = l$ (where l is the length of filament), such that desired state is attained at prescribed fixed final time with minimum energy cost. The presented method has the following properties

i) Decision maker can discretize the times abscissas in an arbitrary way in which the control function is specified. We are not obliged to use equidistance time discretization or the partitioning does not need very fine like as finite difference method for example see [5].

ii) Decision maker is able to prescribe control function on any specific time period that one requires while this is impossible in some methods for example see [8] and references in it.

This means that according to the problem conditions, decision maker is flexible to compute the control function by various means he likes with minimum energy cost.

The outline of this paper is as follow: In Section 2 we give the mathematical formulation of the control problem, review some basic definitions and state the necessary assumptions. In Section 3 a method has been proposed to find optimal control function over a thin elastic rod. In Section 4 some numerical results are given.

2. PROBLEM FORMULATION

We consider the physical domain to be a thin elastic rod of length l. Let $\Omega = (0, l)$ be a bounded open set in $\mathbb{R}$. Let $T > 0$ be a preassigned final time. We set $\mathrm{Q} = \Omega \times (0, T)$. Consider the hyperdiffusion initial–boundary value problem:

$$\frac{\partial}{\partial t} w + a^2 \frac{\partial^4}{\partial x^4} w = 0 \quad \text{in } Q \tag{2.1}$$

The initial condition is

$$w(x, t) = f(x) \quad \text{at } t = 0 \tag{2.2}$$

where $f(x)$ is a real valued function. We assume that for each $t \in (0,T)$ the boundary conditions are

$$\frac{\partial^2}{\partial x^2} w(x,t) = 0 \qquad \text{at } x = 0 \tag{2.3}$$

$$\frac{\partial^2}{\partial x^2} w(x,t) = 0 \qquad at\ x = l \tag{2.4}$$

$$w(x,t) = 0 \qquad \text{at } x = 0 \tag{2.5}$$

$$w(x,t) = u(t) \qquad \text{at } x = l \tag{2.6}$$

where $u(t) \in L^2(0,T)$ is a control function. We assume that $u(0) = u(T) = 0$.

Definition 2.1. Let $\Omega \subset \mathbb{R}^n$ and $s \geq 0$ be a real number. $H^s(\Omega)$ is defined as

$$H^s(\Omega) = [H^r(\Omega), L^2(\Omega)]_\theta,$$

where $[X,Y]_\theta$ denotes the interpolation between two spaces X and Y, r integer, $0 < \theta < 1$ and $(1-\theta)r = s$ (for more details see [14], Chapter 1, Section 9.).

Remark 2.2. Let $s_1, s_2 > 0$. Dual space of $H^{s_2}(\Omega)$ is not necessary identified with an ordinary function space, but, it is an abstract space. We may identify $H^{s_1}(\Omega)$ with a dense subspace of dual space of $H^{s_2}(\Omega)$, in the following manner. Let $u \in H^{s_1}(\Omega)$. Then

$$u_* : \nu \in H^{s_2}(\Omega) \to \int_\Omega u\bar{\nu}\,\mathrm{d}x,$$

is a continuous antilinear form on $H^{s_2}(\Omega)$. Thus, u_* belongs to dual space of $H^{s_2}(\Omega)$. For more details see [14], Chapter 1, Section 12.5.

Theorem 2.3. If the initial state $f(x)$ belongs to dual space of $H^{\frac{3}{2}}(\Omega)$ and the boundary condition $u(t)$ belongs to $L^2(0,T)$, then the solution of the problem (2.1)–(2.6) satisfies

$$w(x,t) \in L^2((0,T); H^{\frac{1}{2}}(\Omega)) \cap H^{\frac{1}{8}}((0,T); L^2(\Omega)).$$

P r o o f. In this case for $\theta = \frac{1}{2}$ and $r = 3$, the dual space of $H^{\frac{3}{2}}(\Omega)$ satisfying in Definition 2.1 and Remark 2.2 exists. For the remainder of proof see reference [14], Chapter 4, Section 15.2. □

We aim at changing the dynamic of the system by acting on the boundary of the domain $(0,l)$. The optimal control problem may be defined in similar way (For example see [20, 24]):

$$\min_{u(t)} \|u(t)\|_{L^2(0,T)} + \|w(x,t,u(t))\|_{L^2(0,T)}.$$

In this paper a different optimal control formulation is considered because the final state is more important than control cost or tracking problem from our point of view. Here, the following optimal control formulation is considered.

Find $u^*(t) \in L^2(0,T)$ such that u^* is the solution of

$$\begin{cases} \min\limits_{u(t)} J(u(t)) \\ \text{s.t.} \quad |w(x,T,u(\cdot))| \le \epsilon \qquad \forall\, x \in (0,l), \end{cases} \tag{2.7}$$

where ϵ is a positive constant that should be given in solving process (see Section 3) and $J(u(t)) = \|u(t)\|^2_{L^2(0,T)}$. The formulation (2.7) guaranties that the final destination will be reached with accuracy ϵ. The null controllability of hyperdiffusion equation is proved by authors in the reference [9]. So, the problem (2.7) is well defined and has at least one solution.

3. METHOD

At first, the classical solution $w(x,t,u(\cdot))$ of (2.1) – (2.6) will be found. In order to find the classical solution we use the following theorems.

Theorem 3.1. Every linear boundary value problem (BVP) with inhomogeneous boundary conditions can be transformed to a BVP with homogeneous boundary conditions.

Proof. See [21]. □

Theorem 3.2. The classical solution of (2.1) – (2.5) and $w(l,t) = 0$ is as follows:

$$w(x,t,u(\cdot)) = \frac{2}{l} \sum_{n=1}^{\infty} \int_0^l f(\xi) \sin(\lambda_n \xi) \exp(-\lambda_n^4 a^2 t)\, \mathrm{d}\xi \sin(\lambda_n x). \tag{3.1}$$

where $\lambda_n = \frac{n\pi}{l},\ n = 1, 2, \ldots.$

Proof. See [23]. □

Theorem 3.3. The classical solution of inhomogeneous BVP (2.1) – (2.6) is as follows:

$$\begin{aligned} w(x,t,u(\cdot)) = \frac{2}{l} \Big[& \sum_{n=1}^{\infty} \int_0^l f(\xi) \sin(\lambda_n \xi) \exp(-\lambda_n^4 a^2 t)\, \mathrm{d}\xi \\ & - \sum_{n=1}^{\infty} \int_0^l \int_0^t \frac{\xi}{l} \frac{\mathrm{d}}{\mathrm{d}\tau} u(\tau) \sin(\lambda_n \xi) \exp(-\lambda_n^4 a^2 (t-\tau))\, \mathrm{d}\tau \mathrm{d}\xi \Big] \sin(\lambda_n x) + \frac{x}{l} u(t). \end{aligned} \tag{3.2}$$

Proof. See Theorem 3.1 and Theorem 3.2. □

The solution $w(x,t,u(\cdot))$ can be approximated by a truncated Fourier series [4]. The constant N arises from the number of retained terms in the Fourier expansion

and specifies the accuracy of the approximation. The positive constant ϵ in optimization problem (2.7) is related to N obviously. The term $w_N(x, T, u(\cdot))$ is defined as follows:

$$w_N(x,T,u(\cdot)) = \frac{2}{l}\sum_{n=1}^{N}\Big[\int_0^l f(\xi)\sin(\lambda_n\xi)\exp(-\lambda_n^4 a^2 T)\,\mathrm{d}\xi - \int_0^l\int_0^T \frac{\xi}{l}\frac{\mathrm{d}}{\mathrm{d}\tau}u(\tau)\sin(\lambda_n\xi)\exp(-\lambda_n^4 a^2(T-\tau))\,\mathrm{d}\tau\mathrm{d}\xi\Big]. \quad (3.3)$$

The constraint $|w(x, T, u(\cdot))| \le \epsilon$ in (2.7) can be replaced by $w_N = 0$ with a large enough N. Therefore, by setting $w_N = 0$ and integration by parts of Eq. (3.3) we have:

$$\sum_{n=1}^{N}\int_0^l f(\xi)\sin(\lambda_n x)\sin(\lambda_n\xi)\exp(-\lambda_n^4 a^2 T)\,\mathrm{d}\xi = -\sum_{n=1}^{N}\int_0^l\int_0^T \frac{\xi}{l}\sin(\lambda_n x)\sin(\lambda_n\xi)\lambda_n^4 a^2 u(\tau)\exp(-\lambda_n^4 a^2(T-\tau))\,\mathrm{d}\tau\mathrm{d}\xi. \quad (3.4)$$

Multiplying both sides of equation (3.4) by appropriate trigonometric function, integrate with respect to x over $[0, l]$ and summing from $n = 1 \ldots N$ we obtain, using orthogonality, the equation

$$\int_0^l f(\xi)\sin(\lambda_n\xi)\exp(-\lambda_n^4 a^2 T)\,\mathrm{d}\xi = -\int_0^l\int_0^T \frac{\xi}{l}\sin(\lambda_n\xi)\lambda_n^4 a^2 u(\tau)\exp(-\lambda_n^4 a^2(T-\tau))\,\mathrm{d}\tau\mathrm{d}\xi \quad n = 1\ldots N. \quad (3.5)$$

The important point to note here is the form of boundary control function that must satisfy in Theorem 2.3 and Eq. (3.3). It is clear that the class of piecewise polynomials as well as piecewise constant functions are appropriate boundary control functions to satisfy theses properties.

3.1. Time discretization

We now define the discrete control problem by discretizing the interval $(0, T)$ into m subdomains at specific points $0 = t_0, t_1, t_2, \ldots, t_m = T$. We assume that $u(t)$ in each subinterval $(t_i, t_{i+1}]$ be specific polynomial $u_{i+1}(t)$ for $i = 0, \ldots, m-2$ and u_m be a specific polynomial on (t_{m-1}, T) such that $u_m(T) = 0$. Note that the control function $u(t)$ that forces in the boundary of the problem belongs to the $L^2(0, T)$ space. The reason is that: This function has exactly $m + 1$ (finite) points of discontinuity, thus, the set of discontinuous points has measure zero in the sense of Lebesgue measure, and by famous theorem in analysis (Lebesgues criterion for Riemann integrability[3]), $u^2(t)$ is integrable.

From (3.5) we get:

$$\int_0^l f(\xi)\sin(\lambda_n\xi)\exp(-\lambda_n^4 a^2 T)\,\mathrm{d}\xi$$
$$= -\int_0^l \sum_{i=0}^{m-1}\int_{t_i}^{t_{i+1}} \frac{\xi}{l}\sin(\lambda_n\xi)\lambda_n^4 a^2 u_{i+1}(\tau)\exp(-\lambda_n^4 a^2(T-\tau))\,\mathrm{d}\tau\mathrm{d}\xi \quad n=1\ldots N. \tag{3.6}$$

Let us now turn our attention to the discrete optimal control problem. One would be expect to find u^* such that

$$u^*(t) = \begin{cases} u_1^*(t) & t_0 < t \le t_1 \\ u_2^*(t) & t_1 < t \le t_2 \\ \vdots & \\ u_m^*(t) & t_{m-1} < t < t_m \end{cases} \tag{3.7}$$

is the optimal solution of problem:

$$\min_{u_i(t)} \sum_{i=1}^{m} \|u_i(t)\|^2_{L^2(0,T)} \tag{3.8}$$

such that N equations in (3.6) satisfy.

Theorem 3.4. If a control function $u(t)$ is given by constant functions on each time's subdomain then N constraints of mathematical programming (3.8) make a convex region, and any local minimum of the mathematical programming (3.8) is a global minimum.

P r o o f. From the norm properties it is easy to show that the cost functional J in (3.8) is a convex functional. Let $u(t)$ be any piecewise constant function in the following form:

$$u(t) = \begin{cases} u_1 & t_0 < t \le t_1 \\ \vdots & \\ u_m & t_{m-1} < t < t_m. \end{cases} \tag{3.9}$$

Thus (3.6) can be presented as follows:

$$\sum_{i=1}^{m} c_{n,i}u_i = b_n \quad n=1\ldots N, \tag{3.10}$$

where

$$c_{n,i} = \int_0^l \int_{t_i}^{t_{i+1}} \frac{\xi}{l}\sin(\lambda_n\xi)\lambda_n^4 a^2 \exp(-\lambda_n^4 a^2(T-\tau))\,\mathrm{d}\tau\mathrm{d}\xi, \tag{3.11}$$

and

$$b_n = \int_0^l f(\xi)\sin(\lambda_n \xi)\exp(-\lambda_n^4 a^2 T)\,\mathrm{d}\xi.$$

It follows from (3.10) that the feasible region of mathematical programming (3.8) is an intersection of N linear hyperplanes, thus it is a convex set. Then since J is a convex functional any local minimum of (3.8) is a global minimum [1]. □

4. NUMERICAL RESULTS

Here we present some numerical results to illustrate the theory developed in the previous sections. We have implemented a prototype version of iterative active-set algorithm in MAPLE in order to obtain computational estimates for the boundary control function $u(t)$. The results were obtained using a personal computer with 3.00 GHz Pentium Dual Processor and 4 GB RAM. In all of the following examples we try to find the optimal function $u^*(t)$ such that it satisfies in Eq. (2.7). According to Section 3 it is proved that, this is equivalent to solve (3.8) subject to N constraints in (3.6), where N stands for the number of constraints. The control is assumed to be constant on each subintervals, i. e., the control function is an unknown piecewise constant function and its values will be calculated in the process of solving the problem. J^* denotes the minimum achieved by solving quadratic programming $\min_{u_i} \sum_{i=1}^{m} u_i^2$ subject to N constraints in (3.10). Note that a single solution of corresponding non-dimensional equation (2.1) using $a^2 = \frac{A}{l^4 \omega \zeta\perp}$, would allow us to solve a wide variety of microswimming problem, because a single parameter $a^2 = \frac{A}{\zeta\perp}$, say, would replace some combination of l, ω, A and $\zeta\perp$, where ω is actuation frequency, A is bending stiffness and $\zeta\perp$ normal drag coefficient [25]. T is the final time, $f(x)$ is the initial state for $x \in [0, 5]$, m is the number of time's subintervals. We assume that $a^2 = 1$ as this is the case where the optimal propulsion is expected [12].

In order to find an upper bound for error, the maximum error

$$MaxError = \max |w_{\mathrm{Exact}}(x, T, u(\cdot)) - w_N(x, T, u(\cdot))|$$

where a_n is nth Fourier coefficient of $w(x, t, u(\cdot))$, is defined. The Euclidean norm

$$Norm2Error = \sum_{i=0}^{60} |w_{\mathrm{Exact}}(x_i, T, u(\cdot)) - w_N(x_i, T, u(\cdot))|^2)^{\frac{1}{2}}$$

is given to show the accumulated error at discrete points $x_i = \frac{il}{60}, \quad i = 0, \ldots, 60$, where w_{Exact} stands for $w_N(x, T, u(\cdot))$ in (3.4) as $N \to \infty$. Here, We consider $w_{\mathrm{Exact}} = w_{50}$.

Error function is defined by

$$Error(x) = w_{\mathrm{Exact}}(x, T, u(\cdot)) - w_N(x, T, u(\cdot)) \quad x \in (0, l) \tag{4.1}$$

The Error function is shown in Figures 1c – 6c and 1d – 6d for various values of N. Figures 1a,- 6a show the convergence for trajectories of $w(x, t, u(\cdot))$ to vanish where $w_{\mathrm{Exact}}(x, T, u(\cdot)) \equiv 0$. Calculated control function $u(t)$ is shown in Figures 1b – 6b.

Example 1. (*Uniform subdomains in time*).
In this example, the time domain is partitioned into subdomains uniformly where $t_i = \frac{iT}{50}$, $i = 0, \ldots, 50$, for $T = 10$ and four initial states, $f(x) = x, x^2, \sin(x)$ and $\frac{1}{\sqrt{1+x}}$. Here, we solve (3.8) with respect to 10 constraints in (3.6). According to Figures 1a, 2a, 3a and 4 the function $w(x, t, u(\cdot))$ for $t = 0.20$, 2.00, 4.00 and 9.00 does not give a good approximation for $w_{\text{Exact}}(x, T, u(\cdot))$. However, $w(x, t, u(\cdot))$ converges to $w_{\text{Exact}}(x, T, u(\cdot))$ as time increases, i. e., near the time $T = 10$, the graph of $w(x, 9.40, u(\cdot))$ fits well with $w_{\text{Exact}}(x, 10, u(\cdot))$ for all $x \in (0, 5)$. Of course as $t \to T = 10$ we will gain better approximation. Control functions on each subinterval are shown in Figures 1b, 2b, 3b and 4b. Although, the profile for $u(t)$ stays similar for various initial states $f(x)$, the values of $u(t)$ differ as it was expected. It is shown in Figures 1c – 4c and 1d – 4d that the error function oscillates finitely in the similar manner. Our computations show that for $N = 10$ we reach to the moderate accuracy over all points in the domain $0 \leq x \leq 5$.

The log plot of $MaxError$ and $Norm2Error$ for different values of N are presented in Figures 7 and 8, respectively. It is shown that the maximum and Euclidean norm for the error decreases very fast and stays the same for $N \geq 6$.

Example 2. (*Non-uniform subdomains in time*).
Let T=10, $f(x) = x$, N=10, l=5 and $m = 50$. In this example, the following non-uniform partitioning in time is considered.
$t_i = \frac{iT}{m}$, $i = 0, \ldots, 20$; $t_{21} = 4.5$, $t_{22} = 5.2$; $t_i = 5.2 + (i - 22)\frac{(T-5.2)}{28}$, $i = 22, \ldots, 50$.
Numerical computation for optimization problem (3.8) with respect to the above data gives: J^*= 102.256 where $MaxError = 2.020 \times 10^{-44}$. The maximum error happens at a point near to $x = 5$.

According to Figure 5a the function $w(x, t, u(\cdot))$ converges to $w(x, T, u(\cdot))$ as time increases. In Figure 5b the control function $u(t)$ is depicted. Here, the profile of control function stays similar to uniform time partitioning unless that its values differ in those subintervals that are not chosen uniformly. Figures 5c and 5d represent the behavior of function $Error(x)$ for every $x \in (0, 5)$ where $N = 6$ and $N = 10$ respectively.

Example 3. (*Non-uniform subdomains in time and a preassigned value for $u(t)$*).
In this example, we suppose that the value of control function $u(t)$ at a specified time subdomain is preassigned (here it is chosen to be zero). Consider Example 2 and let control function to be zero at $4.5 \leq t \leq 5.2$ i. e., $u_{22} = 0$. The following results are computed: J^*=131.261, $MaxError = 2.484 \times 10^{-44}$.

In Figure 6a it is shown that the function $w(x, t, u(\cdot))$ does not fit to $w(x, T, u(\cdot))$ at times close to zero. However, $w(x, t, u(\cdot))$ converges to $w(x, T, u(\cdot))$ as time increases. In Figure 6b the function $u(t)$ is depicted, it is shown that for $4 \leq t \leq 5$ the computed value for $u(t)$ is -3.968.

In Table 2, preassigned values for u_{22} =-5.000, -4.753, -4.000, -3.000, 0.000, 3.000, 4.000, 4.753, 5.000, inside interval $(4.5, 5.2]$ are considered. The corresponding values for u_{21} are computed in the fixed interval $(4, 4.5]$. Moreover, the values of $u_1, \ldots, u_{20}$ and $u_{23}, \ldots, u_{50}$ are computed and their values are shown in Figure 6b for $u_{22} =$

0.000. In this table we show that if one choose $u_{22} = -4.753$ then for $f(x) = x$, J^* has the minimal value. This coincide with the results found in Example 2. (See also, Table 1). This means that if the decision maker has some information about control function on some specific time intervals, he will be able to make better decision in order to gain minimal energy function.

Table 1. Numerical results for some various initial states in Examples 1, 2 and 3 for $T = 10$, $m = 50$, N=10 and l=5.

Example	$f(x)$	J^*	$MaxError$	$Norm2Error$	CPU time (s)
1	x	120.172	1.313×10^{-19}	3.065×10^{-20}	24.015
2	x	102.256	2.020×10^{-44}	1.524×10^{-44}	24.800
3	x	131.261	2.484×10^{-44}	1.874×10^{-44}	25.703
1	x^2	1062.587	1.562×10^{-19}	9.113×10^{-20}	26.012
2	x^2	904.165	6.008×10^{-44}	4.533×10^{-44}	34.250
3	x^2	1160.631	7.386×10^{-44}	5.731×10^{-44}	30.047
1	$\sin(x)$	1.759	6.570×10^{-20}	3.834×10^{-21}	26.359
2	$\sin(x)$	1.600	2.528×10^{-45}	1.907×10^{-45}	38.844
3	$\sin(x)$	2.054	3.107×10^{-45}	2.345×10^{-45}	27.656
1	$\frac{1}{\sqrt{x+1}}$	5.984	1.172×10^{-20}	6.837×10^{-21}	29.313
2	$\frac{1}{\sqrt{x+1}}$	5.092	4.508×10^{-45}	3.402×10^{-45}	48.516
3	$\frac{1}{\sqrt{x+1}}$	6.536	5.543×10^{-45}	4.182×10^{-45}	31.266

Table 2. Numerical results for some various preassigned values for u_{22} in Example 3, where u_{21} and u_{22} are non-uniform subdomains and the other subdomains are such that $t_{i+1} - t_i = 0.2$, for $i = 0, \ldots, 20$, and $t_{i+1} - t_i = 0.1714285714$, for $i = 23, \ldots, 50$.

u_{22}	u_{21}	J^*	$MaxError$	$Norm2Error$	CPU time (s)
-5.000	-3.046	102.334	1.880×10^{-44}	1.418×10^{-44}	29.156
-4.753	-3.092	102.256	1.966×10^{-44}	1.524×10^{-44}	24.953
-4.000	-3.231	102.985	1.966×10^{-44}	1.483×10^{-44}	28.890
-3.000	-3.415	106.203	2.094×10^{-44}	1.580×10^{-44}	27.256
0.000	-3.968	131.261	2.484×10^{-44}	1.874×10^{-44}	25.703
3.000	-4.522	179.425	2.863×10^{-44}	2.160×10^{-44}	24.968
4.000	-4.706	200.614	2.906×10^{-44}	2.193×10^{-44}	25.703
4.753	-4.845	218.276	1.966×10^{-44}	2.232×10^{-44}	25.000
5.000	-4.891	224.370	3.162×10^{-44}	2.386×10^{-44}	28.515

In Figures 6c and 6d it is observed that the behavior of $Error(x)$ is similar for $N \geq 6$, it gets better as N increases. Comparison between Figures 5c, 6c) and 5d, 6d show the behavior of $Error(x)$ does not change in Examples 2 and 3 for $N = 6$ and $N = 10$ respectively, the J^* will differ (see Table 1).

5. CONCLUSION

In this paper, we have presented a direct approach for solving hyperdiffusion optimal control problem. Fourier expansion have been used to generate the optimal solution of control problem. Closed analytical form solution of homogeneous hyperdiffusion problem is introduced. In the nonhomogeneous case the closed analytical form is proposed. It is proved that for piecewise constant control functions we deal with convex programming problem and therefore every local minimum of the corresponding convex program is a global minimum.

The effect of various initial state functions is discussed in Example 1. It is shown that the norm of control function $u(t)$ has a direct relation with the initial state $f(x)$, (see Table 1). As it is shown in Table 1, the non-uniform subdivision in time will give better minimal energy function, however it needs more CPU time as it was expected.

In Figures 9 and 10 it is shown that for $N = 2$, 3, 4, 5, and 6, we have almost the same amount of error for uniform, non-uniform and preassigned values, while for $N > 6$ the non-uniform subdivision in time will give better result.

The numerical results for various examples show that the solutions perform successful convergence to the correct solution and it verify the theory in Section 3, (see Theorem 3.4).

(Received November 15, 2009)

REFERENCES

[1] S. Boyd and L. Vandenberghe: Convex Optimization. Cambridge University Press 2004.

[2] C. Brennen and H. Winet: Fluid mechanics of propulsion by cilia and flagella. Ann. Rev. Fluid Mech. *9* (1977), 339–398.

[3] F. Burk: Lebesgue Measure and Integration: An Itroduction. John Wiley & Sons, 1998.

[4] C. Canuto, M. Y. Hussaini, A. Quarteroni, and T. A. Zang: Spectral Methods: Fundamentals in Single Domains. Springer-Verlag, 2006.

[5] G. Dimitriu: Numerical approximation of the optimal inputs for an identification problem. Internat. J. Comput. Math. *70* (1998), 197–209.

[6] R. Dreyfus, J. Baudry, M. L. Roper, M. Fermigier, H. A. Stone, and J. Bibette: Microscopic artificial swimmers. Nature *437* (2005), 862–865.

[7] F. Fahroo: Optimal placement of controls for a one-dimensional active noise control problem. Kybernetika *34* (1998), 655–665.

[8] M. H. Farahi, J. E. Rubio, and D. A. Wilson: The optimal control of the linear wave equation. Internat. J. Control *63* (1996), 833–848.

[9] H. Heidari and A. Malek: Null boundary controllability for hyperdiffusion equation. Internat. J. Appl. Math. *22* (2009), 615–626.

[10] G. Ji and C. Martin: Optimal boundary control of the heat equation with target function at terminal time. Appl. Math. Comput. *127* (2002), 335–345.

[11] Y. W. Kim and R. R. Netz: Pumping fluids with periodically beating grafted elastic filaments. Phys. Rev. Lett. *96* (2006), 158101.

[12] E. Lauga: Floppy swimming: Viscous locomotion of actuated elastica. Phys. Rev. E. *75* (2007), 041916.

[13] E. Lauga and T. R. Powers: The hydrodynamics of swimming microorganisms. Rep. Prog. Phys. *72* (2009), 096601.

[14] J. L. Lions and E. Magenes: Non-homogeneous Boundary Value Problem and Applications. Springer-Verlag, 1972.

[15] K. E. Machin: The control and synchronization of flagellar movement. Proc. Roy. Soc. B. *158* (1963), 88–104.

[16] K. E. Machin: Wave propagation along flagella. J. Exp. Biol. *35* (1985), 796–806.

[17] B. S. Mordukhovich and J. P. Raymond: Optimal boundary control of hyperbolic equations with pointwise state constraints. Nonlinear Analysis *63* (2005), 823–830.

[18] H. M. Park, M. W. Lee, and Y. D. Jang: An efficient computational method of boundary optimal control problems for the burgers equation. Comput. Meth. Appl. Mech. Engrg. *166* (1998), 289–308.

[19] E. M. Purcell: Life at low Reynolds number. Amer. J. Phys. *45* (1977), 3–11.

[20] S. A. Reju and D. J. Evans: Computational results of the optimal control of the diffusion equation with the extended conjugate gradient algorithm. Internat. J. Comput Math. *75* (2000), 247–258.

[21] K. Rektorys: Variational Methods in Mathematics, Sciences and Engineering. D. Reidel Publishing Company, 1977.

[22] K. Sakthivel, K. Balachandran, R. Sowrirajan, and J-H. Kim: On exact null controllability of black scholes equation. Kybernetika *44* (2008), 685–704.

[23] C. H. Wiggins, D. Riveline, A. Ott, and R. E. Goldstein: Trapping and wiggling: Elastohydrodynamics of driven microfilaments. Biophys. J. *74* (1998), 1043–1060.

[24] P. Williams: A Gauss–Lobatto quadrature method for solving optimal control problems. ANZIAM *47* (2006), C101–C115.

[25] T. S. Yu, E. Lauga, and A. E. Hosoi: A experimental investigations of elastic tail propulsion at low Reynolds number. Phys. Fluids *18* (2006), 091701.

Hanif Heidari, Department of Applied Mathematics, Faculty of Mathematical Sciences, Tarbiat Modares University, P.O.Box 14115-134, Tehran. Iran.

e-mail: h.heidari@modares.ac.ir

Alaeddin Malek, Department of Applied Mathematics, Faculty of Mathematical Sciences, Tarbiat Modares University, P.O.Box 14115-134, Tehran. Iran.

e-mail: mala@modares.ac.ir

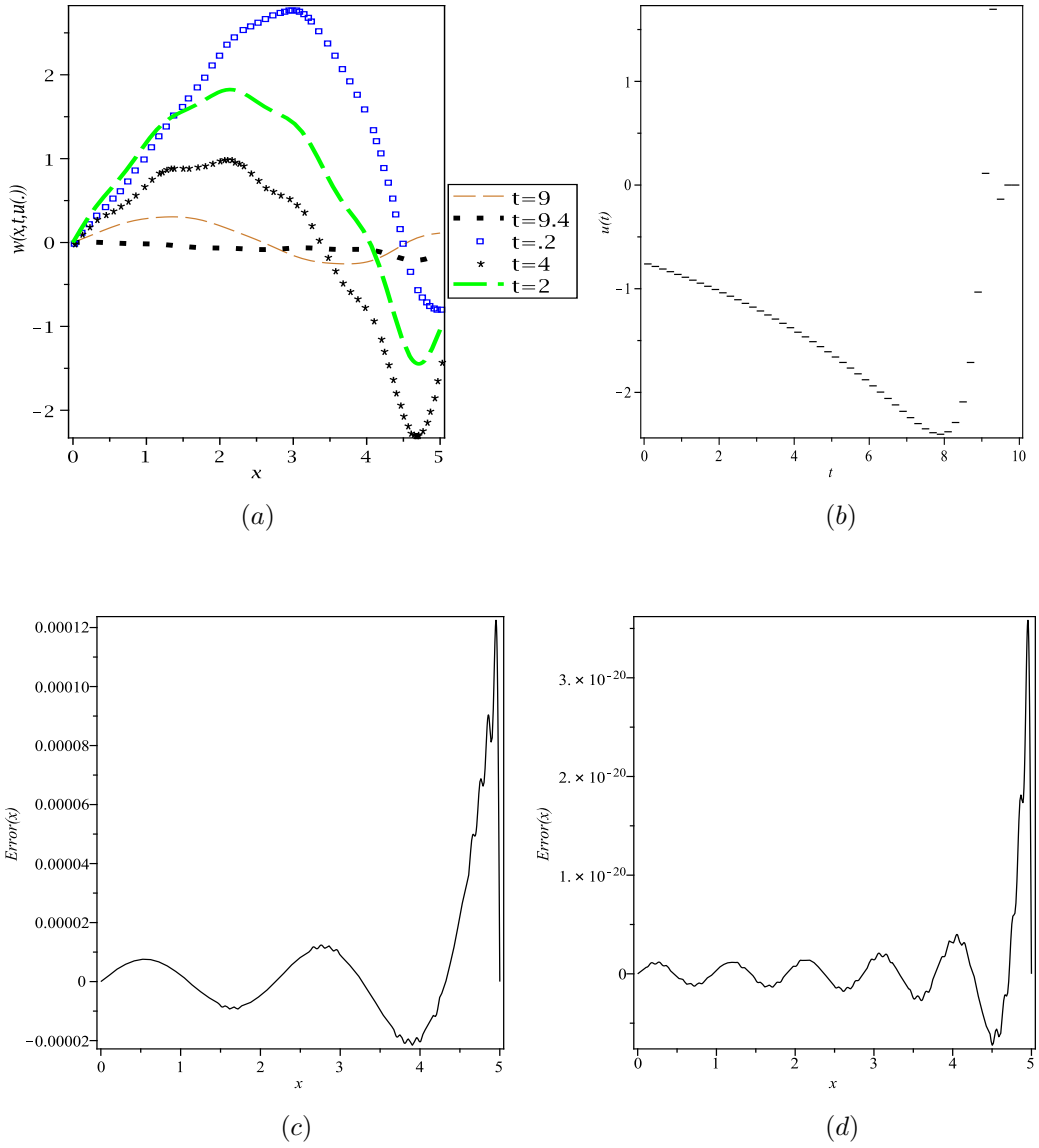

Fig. 1. $f(x) = x$ in Example 1
1a: State of $w(x, t, u(\cdot))$ at times t=0.20, 2.00, 4.00, 9.00, 9.40.
1b: Profile of piecewise constant optimal control calculated by the direct illustrated method.
1c: Plot of function $Error(x)$ for N=4.
1d: Plot of function $Error(x)$ for N=10.

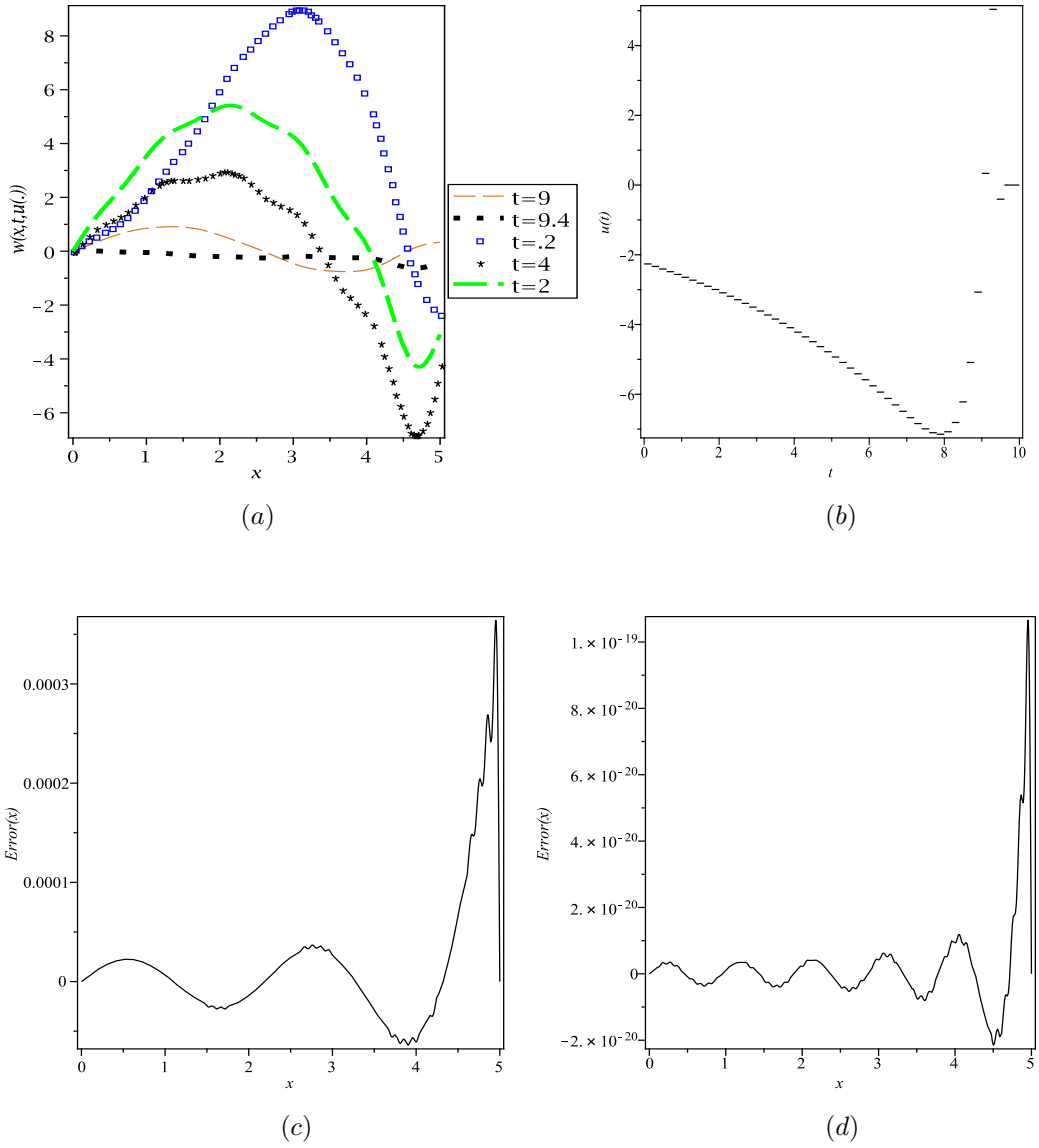

Fig. 2. $f(x) = x^2$ in Example 1
2a: State of $w(x, t, u(\cdot))$ at times t=0.20, 2.00, 4.00, 9.00, 9.40.
2b: Profile of piecewise constant optimal control calculated by the direct illustrated method.
2c: Plot of function $Error(x)$ for N=4.
2d: Plot of function $Error(x)$ for N=10.

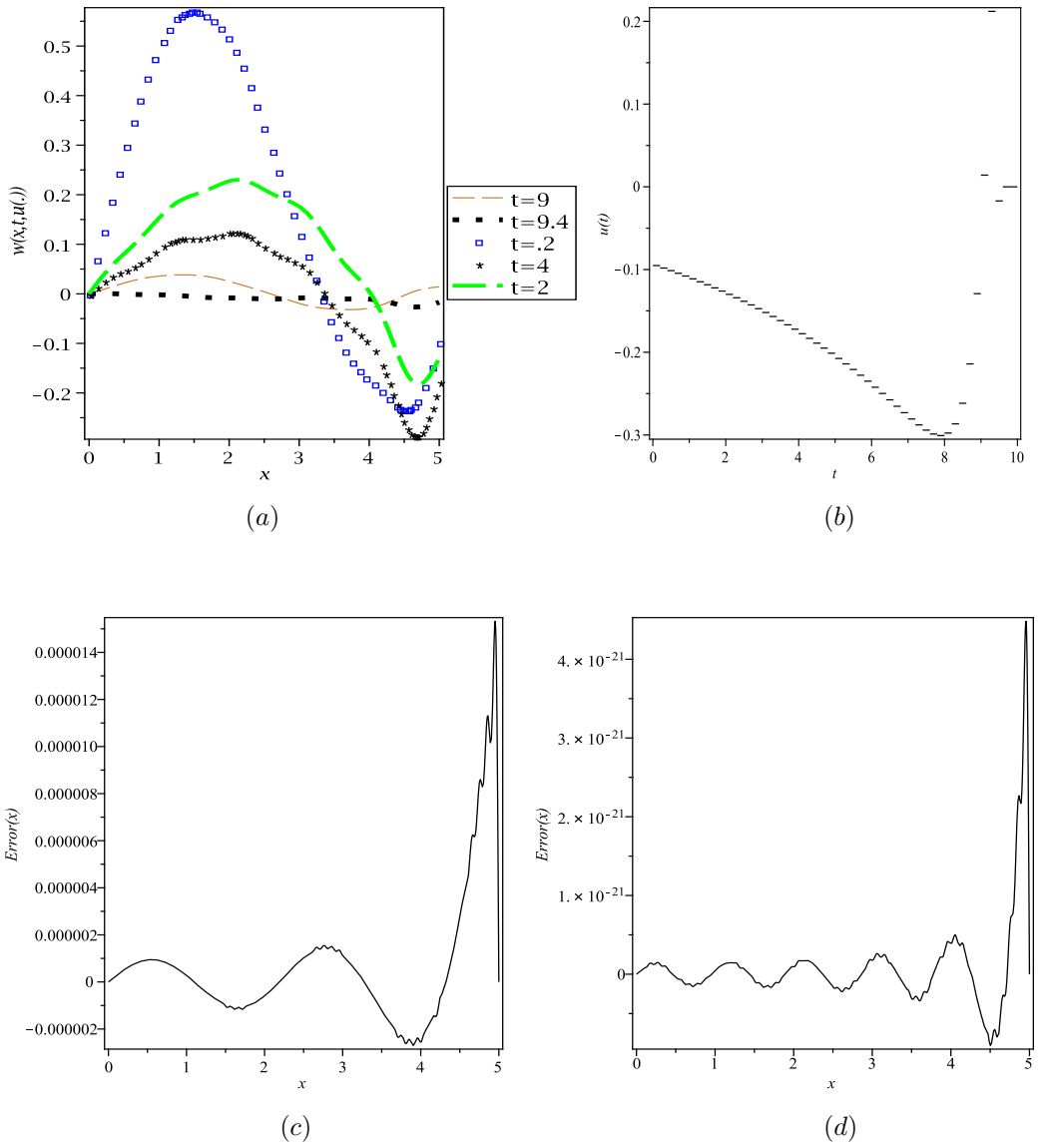

Fig. 3. $f(x) = \sin(x)$ in Example 1
3a: State of $w(x, t, u(\cdot))$ at times t=0.20, 2.00, 4.00, 9.00, 9.40.
3b: Profile of piecewise constant optimal control calculated by the direct illustrated method.
3c: Plot of function $Error(x)$ for N=4.
3d: Plot of function $Error(x)$ for N=10.

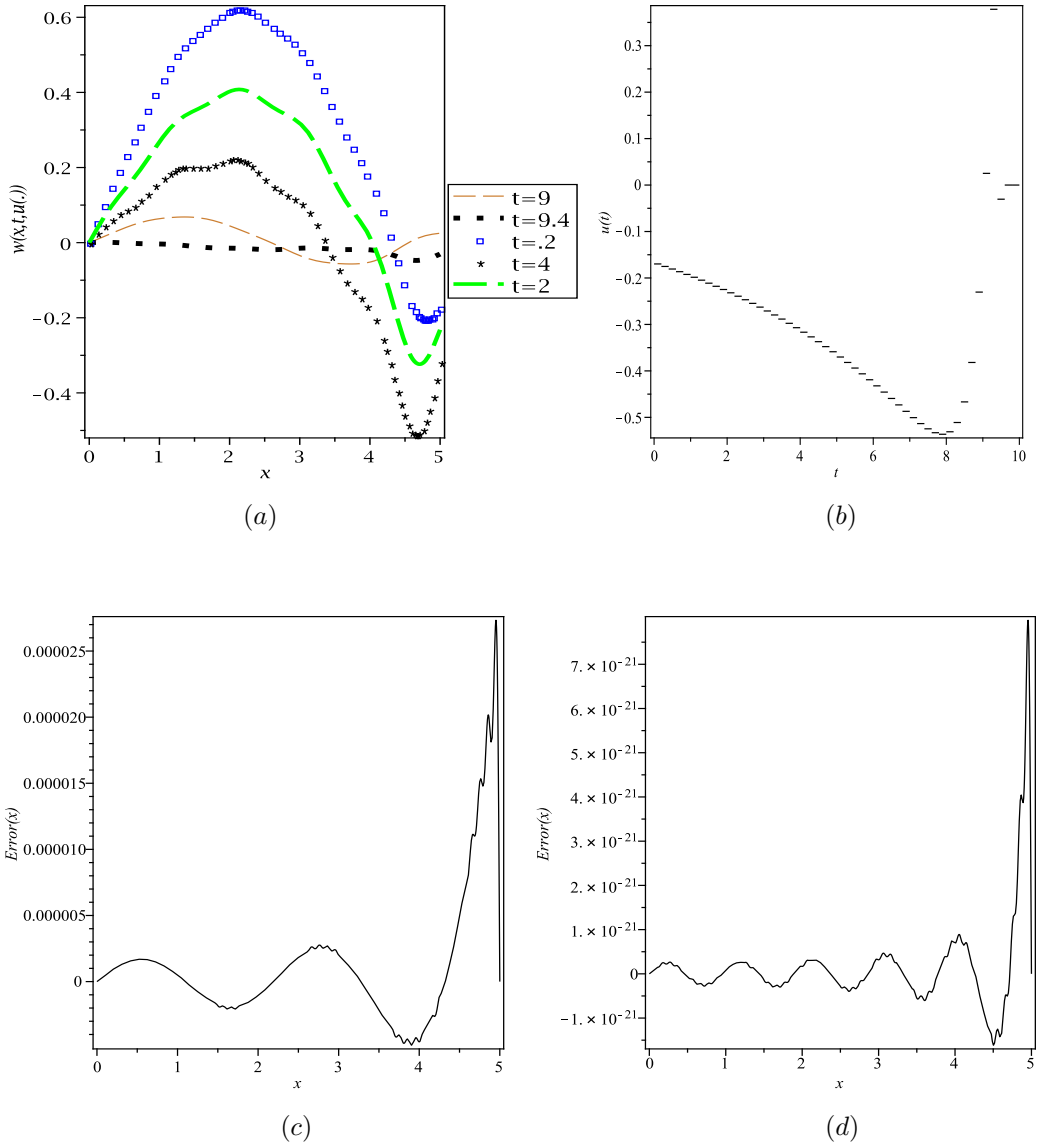

Fig. 4. $f(x) = \frac{1}{\sqrt{1+x}}$ in Example 1
4a: State of $w(x,t,u(\cdot))$ at times t=0.20, 2.00, 4.00, 9.00, 9.40.
4b: Profile of piecewise constant optimal control calculated by the direct illustrated method.
4c: Plot of function $Error(x)$ for N=4.
4d: Plot of function $Error(x)$ for N=10.

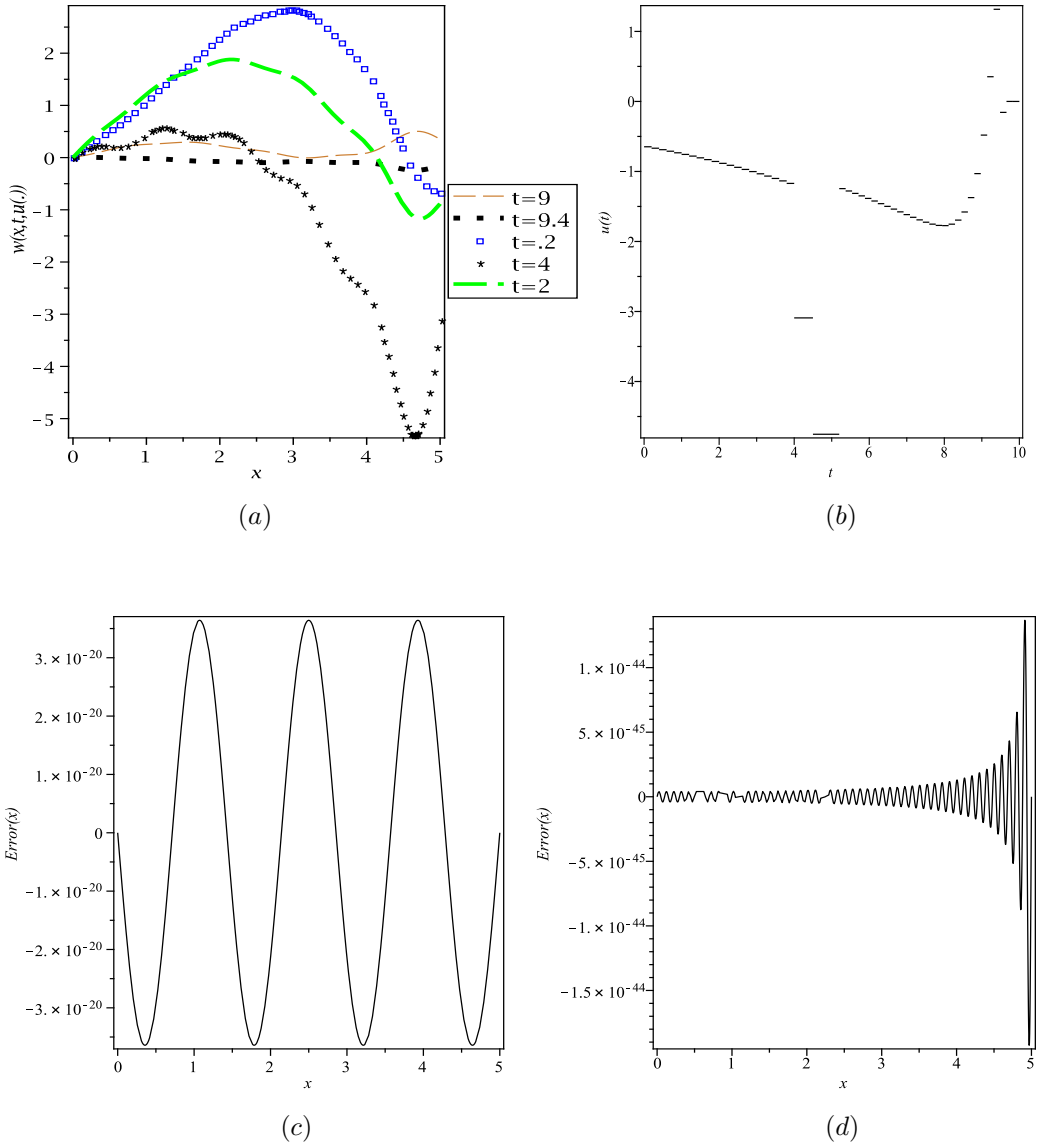

Fig. 5. $f(x) = x$ in Example 2
5a: State of $w(x, t, u(\cdot))$ at times t=0.20, 2.00, 4.00, 9.10, 9.48.
5b: Profile of piecewise constant optimal control calculated by the direct illustrated method.
5c: Plot of function $Error(x)$ for N=6.
5d: Plot of function $Error(x)$ for N=10.

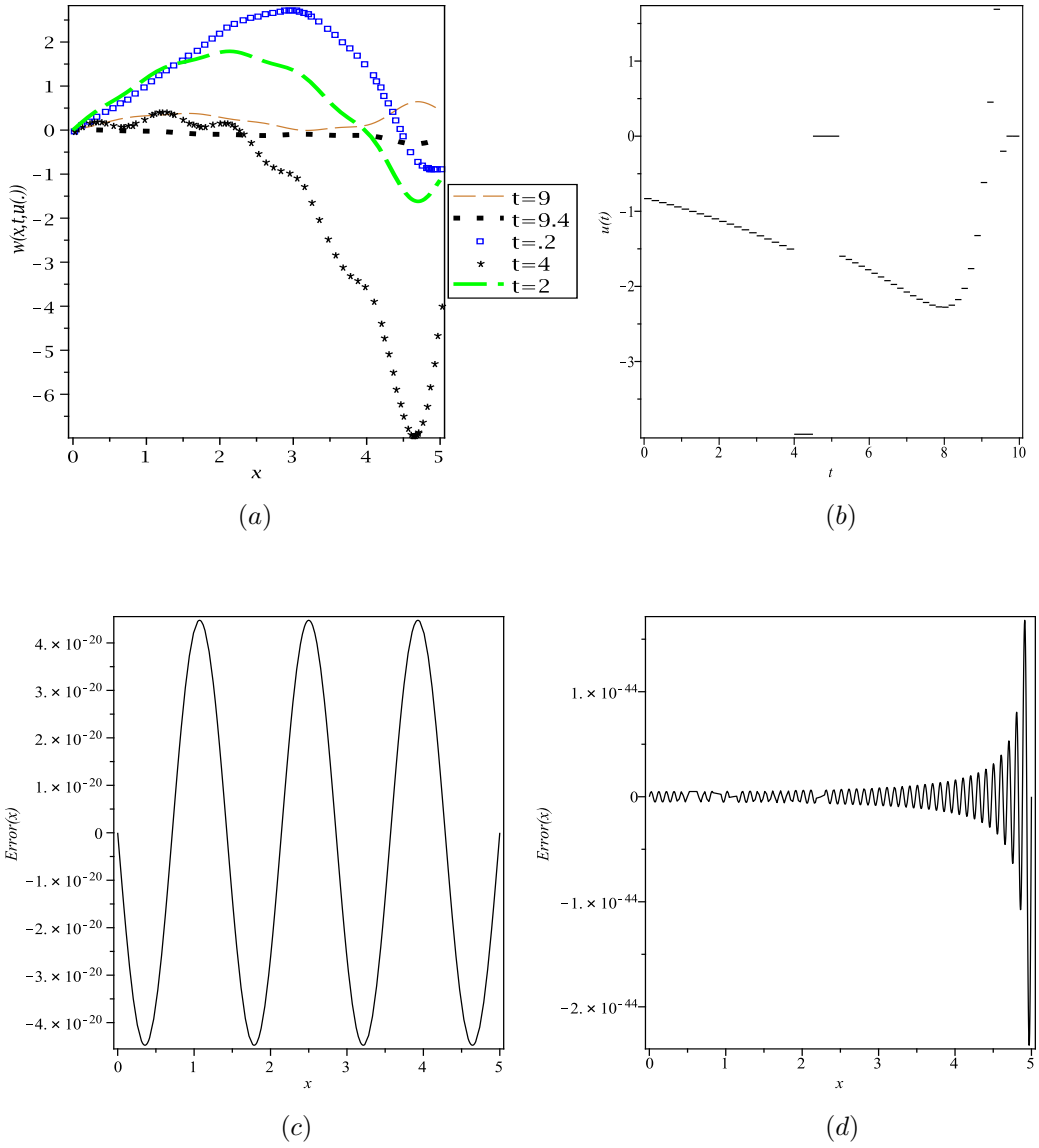

Fig. 6. $f(x) = x$ in Example 3
6a: State of $w(x, t, u(\cdot))$ at times t=0.20, 2.00, 4.00, 9.10, 9.48.
6b: Profile of piecewise constant optimal control calculated by the direct illustrated method.
6c: Plot of function $Error(x)$ for N=6.
6d: Plot of function $Error(x)$ for N=10.

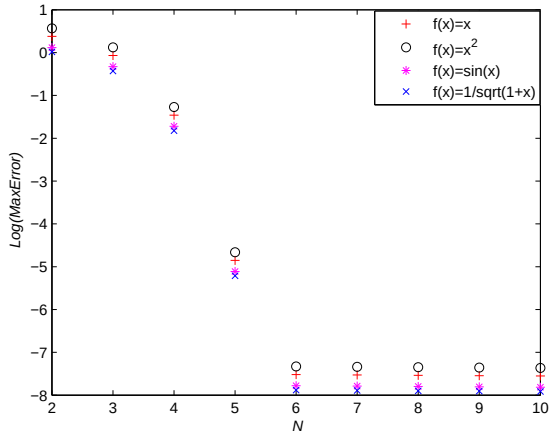

Fig. 7. Logarithm of maximum error at some various values of N and initial states for uniform time subdomains partitioning in Example 1.

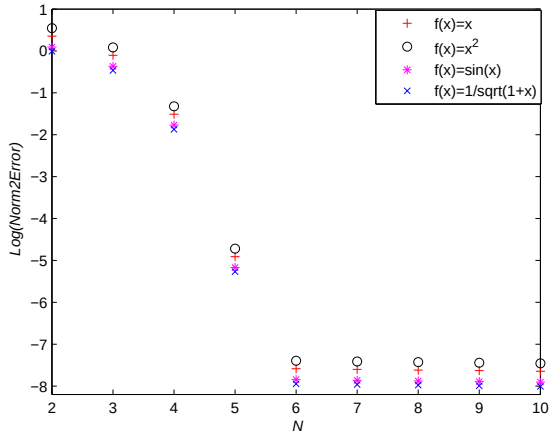

Fig. 8. Logarithm of Euclidean norm error at discrete points $x_i = \frac{il}{60} \quad i = 0, \ldots, 60$ at some various values of N for uniform time subdomains partitioning in Example 1.

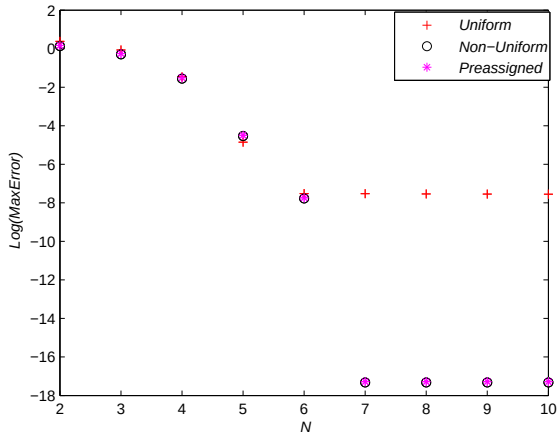

Fig. 9. Logarithm of maximum error at some various values of N for uniform and non-uniform time subdomains partitioning where uniform refers as Example 1, for $f(x) = x$, non-uniform refers as Example 2, and preassigned refers as Example 3.

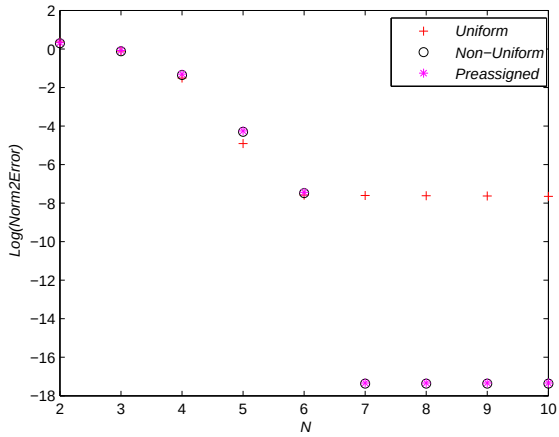

Fig. 10. Logarithm of Euclidean norm error at some various values of N for uniform and non-uniform time subdomains partitioning where uniform refers as Example 1, for $f(x) = x$, non-uniform refers as Example 2, and preassigned refers as Example 3.